



Nanostructures for all-polymer microfluidic systems

Maria Matschuk*, Henrik Bruus, Niels B. Larsen

Department of Micro- and Nanotechnology, Technical University of Denmark, Building 345 East, DK-2800 Kongens Lyngby, Denmark

ARTICLE INFO

Article history:

Received 15 September 2009
Received in revised form 25 November 2009
Accepted 27 November 2009
Available online 3 December 2009

Keywords:

Injection molding
Nanostructures
Electron beam lithography
Electroforming
Nickel mold
Polymer
Cyclic olefin copolymer
Topas

ABSTRACT

We present a process for fabricating nanostructured surfaces with feature sizes down to at least 50 nm and aspect ratios of 1:1 by injection molding. We explored the effects of mold coatings and injection molding conditions on the final nanostructure quality. A plasma-polymerized fluorocarbon based antistiction coating was found to improve the replication fidelity (shape and depth) of nanoscale features substantially. Arrays of holes of 50 nm diameter/35 nm depth and 100 nm/100 nm diameter, respectively, were mass-produced in cyclic olefin copolymer (Topas 5013) by injection molding. Polymer microfluidic channel chip parts resulted from a separate injection molding process. The microfluidic chip part and the nanostructured chip part were successfully bonded to form a sealed microfluidic system using air plasma assisted thermal bonding.

© 2009 Elsevier B.V. All rights reserved.

1. Introduction

Recent years have shown an increasing need for mass-production of nanostructures with high-precision, for e.g. antireflection [1,2] or antistiction coatings [3], optical data storage (e.g. Blu-ray disk) and for biomaterial applications. Therapeutic uses of human mesenchymal stem cells are of immense current interest, and their differentiation into particular cell lineages has recently been demonstrated to depend sensitively on the order of nanoscopic hole arrays [4]. We aim at integrating this type of cellular control in disposable microfluidic chip units, which calls for cost-effective production of the required nanostructures and their stable integration in a microfluidic system. Injection molding is the industrially preferred technology platform for low cost fabrication of polymer items in large numbers, but the technology has not yet been established for fabricating nanostructures of higher aspect ratios (≥ 1) in all relevant polymer materials.

Molding of polymer nanostructures down to 25 nm in width has been reported using injection molding [5–8]. Schiff et al. demonstrated the injection molding of 25 nm wide and 40 nm deep structures [8], although the replication uniformity is sub-optimal even over a small area ($<4 \mu\text{m}^2$). Most injection molded features have been of height-to-width aspect ratios below one [5,6,9]. Sub-100 nm-features with aspect ratios larger than one and uniform shape over a larger area are difficult to realize by injection molding,

especially in the widely and increasingly used cyclic olefin copolymer (COC). In fact, COC has been shown to replicate sub- μm structures worse than materials commonly used for injection molding, like polycarbonate or PMMA [7]. Injection molding of sub-100 nm surface structures of aspect ratio one or larger in COC has not been reported to our knowledge.

Phenomena at nanometer length scales are strongly influenced by interfacial effects, including wettability and friction, due to the increase in surface-to-volume ratio for decreasing dimensions. Inability of the polymer melt to fill nanoscale cavities during injection will limit the resolution of injection molding. This may be caused by insufficient wetting of the polymer melt on the mold surface. Given adequate cavity filling, inability of the solidified polymer to leave the nanoscale cavity during demolding may lead to nanostructural failure. Demolding exposes the molded polymer nanostructures to high frictional forces compared to their relatively low mechanical stability which may lead to their break-off from the bulk of the molded polymer. Optimal molds and molding conditions should therefore target proper filling and ease of release from the nanocavities of the mold.

The application of antistiction coatings on the mold can reduce frictional forces between mold and polymer during demolding. Antistiction coatings of fluorocarbon-silanes [10], fluorocarbons [11] or self-assembled monolayers [12] have been shown to improve the replication fidelity of hot-embossed features. However, antistiction coatings have not been tested as extensively for injection molding. The pressure on the polymer melt at the time of its initial contact with the (cold) mold surface is very low in injection

* Corresponding author.

E-mail address: maria.matschuk@nanotech.dtu.dk (M. Matschuk).

molding, in contrast to embossing processes where the polymer melt is forced into the (hot) mold cavities by the applied pressure. This implies that nanostructure filling in injection molding may be strongly dependent on the interfacial energy of the mold and the polymer melt. Thus, a low surface energy antistiction coating could limit the filling of nanoscale cavities in the mold due to insufficient wetting of the coating by the polymer melt [13].

We find that optimization of molding parameters only lead to slight improvements in replication quality (feature depth and width). In contrast, the application of an antistiction coating results in major improvements in replication quality, improvements that are largely insensitive to variations in the molding parameters. We were able to mass-produce (>500 pieces) 100 nm wide and deep holes with high replication fidelity and uniformity over a large area (0.5 mm²). Furthermore, we demonstrate that polymeric nanostructures can be thermally bonded to polymeric microfluidic systems without deformation of the nanostructures and with very limited deformation of the microfluidic channels.

2. Experimentals

Micro- and nanostructured surface topographies were injection molded in cyclic olefin copolymer, Topas 5013L-10 (TOPAS Advanced Polymers), using a commercial injection molder, ENGEL Victory 80/45 (ENGEL Austria). A conventional injection molding (IM) process consists of polymer melting, filling of the mold cavity, packing, cooling, and part release. The structures were molded with various parameter sets to maximize the replication fidelity (width, depth, and shape). The influence of mold temperature (115–140 °C), melt temperature (270–290 °C), injection velocities (2.0–8.0 cm³/s), and holding pressure (300–600 bars) were investigated. The parts were demolded and ejected at a mold temperature of 55 ± 5 °C. To assure stabilization of the IM process, at least 25 pieces were injection molded for each set of parameters and only the final pieces used in the quality assessment.

The mold consists of a base plate with exchangeable insert. Micro- and nanostructured inserts were produced as a replica relief by electroplating of nickel on a silicon wafer based master structure. Microstructures were formed by UV lithography in a negative photoresist, SU-8 2075 (MicroChem, Newton, MA), spin-casted on a silicon wafer. Nanostructured holes of nominal lateral dimensions of 50 nm or 100 nm, respectively, a pitch of two times the structure width, and aspect ratios of 1:1–1:2 (Fig. 1) were fabricated by electron beam lithography (JBX-9300FS, Jeol) in an electron sensitive polymer, ZEP520A (Zeonrex Electronic Chemicals). Subsequently, structures formed in SU-8 or silicon were coated with a monolayer of FDTs (CAS No. 78560-44-8), deposited by a MVD 100 Molecular Vapor Deposition System (Applied Microstructures) to support the release of master and nickel shim. The electroplating process is similar to that described by Mönkkönen et al. [7]. The micro- and nanostructured master were sputter-coated with 100 nm nickel-vanadium composite (7 wt.% vanadium) and subsequently electroplated in a galvanic nickel bath to a final thickness of about 300 μm (DVD Norden A/S, Denmark). The resulting nickel shim presented a replica relief of the original master relief. A set of nickel molds was coated with 10 nm fluorocarbon polymer by plasma-polymerization of CHF₃ monomer using a Plasmatherm 740 RIE system (Unaxis, St. Petersburg, FL).

Microfluidic chip parts and nanostructure chip parts were thermally bonded after activation of both chip parts in an air plasma (0.6 mbar, 50 W, 30 s). Bonding proceeded at an applied pressure and temperature of 7.6 bars and 123 °C for 15 min.

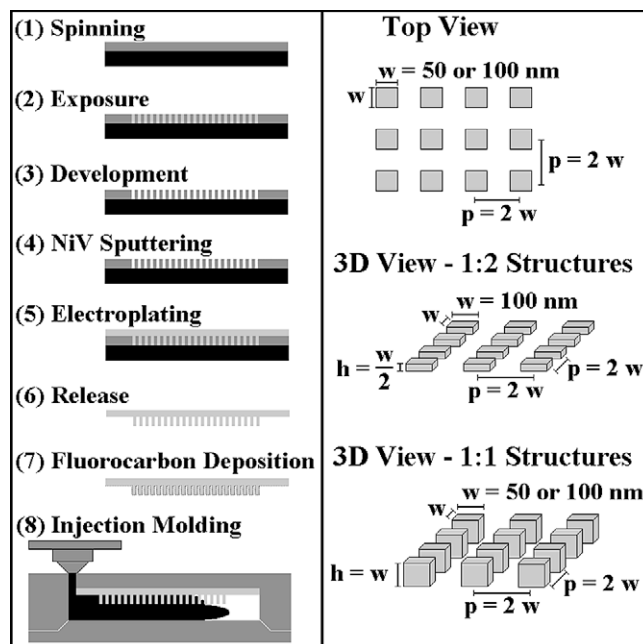


Fig. 1. (Left) Schematic diagram of the mold fabrication and replication, and (right) 2D and 3D sketch of fabricated nickel mold inserts: pillar array structures with features of w = width, h = height, p = pitch.

3. Results and discussion

3.1. Mold fabrication

Microfluidic channels of 200 μm in width and 25–100 μm in height were successfully fabricated in the negative photoresist SU-8 and replicated with high fidelity in nickel to form a mold insert for fabrication of a microfluidic chip part.

The fabrication of nickel molds containing 50 and 100 nm wide pillars, respectively, was successfully realized with pillars having aspect ratios of 1:2–1:1. Patterned surfaces were analyzed at different areas using atomic force microscope (AFM) and scanning electron microscope (SEM). All nanostructures written into ZEP520A were of high quality after development, i.e. without undercuts and of homogenous size over the whole patterned area. No substantial nano- or micro-scaled defects were observed. The electroplating replicated all nanostructures with high fidelity (shape and depth) into a nickel mold insert (Fig. 2a).

3.2. Injection molding

Micro- and nanostructured surface topographies were successfully injection molded in Topas 5013. Microstructures of 200 μm width and 25–100 μm in height were replicated. Randomly occurring micro-scaled cracks disappeared after application of an antistiction layer based on plasma-deposited fluorocarbon on the nickel mold. No effect on the replication fidelity (shape or depth) could be seen compared to uncoated nickel molds.

Holes of widths from 50 to 100 nm were replicated in Topas 5013 using an uncoated nickel mold. The overall surface of nanostructured areas molded on nickel molds without antistiction coating often showed regular nanoscale defects and distortions (Fig. 2b) and randomly distributed large-scale defects. Large-scale defects were most probably caused by stiction of polymer to the mold during demolding. Polymer contamination on the nickel mold, deposited during the first molding cycles, remained on the mold surface even after further molding cycles. The additional

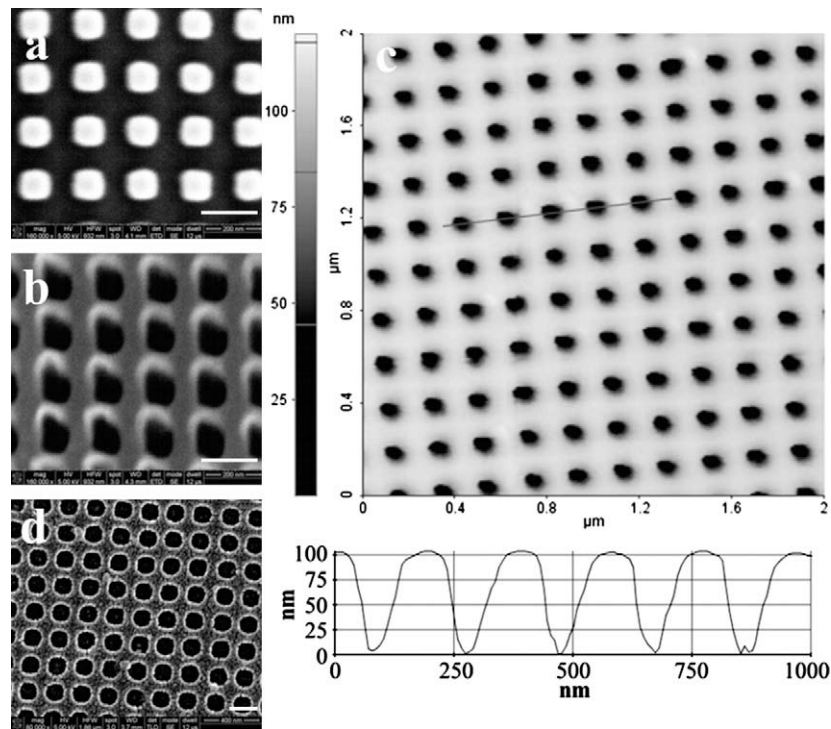


Fig. 2. Scanning electron micrograph of 100 nm wide and deep holes: (a) nickel mold, (b) polymer replica thereof molded without antistiction coating, and (c) atomic force micrograph with line profile of polymer replica molded with antistiction coating (same mold, scan size: $2 \times 2 \mu\text{m}^2$, profile length: $1 \mu\text{m}$) and (d) scanning electron micrograph after their forced debonding from microfluidic structures. Scale bars represent 200 nm.

motif of contamination was transferred with high fidelity to subsequently molded objects. Injection molding of 50 nm wide holes resulted in deformed elongated shapes of depths of about 10 nm (mold depth 100 nm). The maximum achievable depth of 100 nm wide holes using uncoated nickel molds was not explored since the lateral shapes obtained were heavily distorted and therefore irrelevant as structural targets.

In contrast, we were able to replicate 50–100 nm wide holes with homogenous shape and without observable macroscopic defects over the whole structured area in Topas 5013, using a fluorocarbon based antistiction coating plasma-polymerized from CHF_3 monomers. The application of a fluorocarbon based antistiction coating was tested with the known caveat that they may limit the filling of nanoscaled cavities in the mold [13]. A layer of 10 nm fluorocarbon on a nickel mold surface enhances the replication fidelity of nanoscaled structures substantially without reducing the replication depth. The replication quality was improved and large-scale defects of the overall patterned surface were fully removed. 50 nm wide structures were replicated with a maximum depth of 35 nm (mold with 50 nm high pillars) while 100 nm wide structures could be replicated with full depth of 105 ± 5 nm (mold with 105 ± 5 nm high pillars) (Fig. 2c). X-ray photoelectron spectroscopy was employed to probe for inadvertent transfer of the fluorocarbon coating on the nickel mold to the injection molded pieces. No traces of fluorine were observed on molded items (data not shown). No degradation of the antistiction layer was observed, even after hundreds of injection molded pieces.

Optimization of process parameters resulted in the highest replication fidelity for width and depth at a holding pressure of 400 bars and injection velocity of $4 \text{ cm}^3/\text{s}$ (Fig. 3). The replication depth increases with increasing holding pressure up to 400 bars and decreases for higher pressures. Holes replicated with up to 400 bars were about 100 ± 5 nm wide while higher holding pressures caused widening of the structures by about 40%. Holding

pressure is required to compensate for polymer shrinkage during cooling (0.4–0.7%). However, the application of excessive pressure condenses the bulk polymer leading to stress-related deformation of its topography, e.g. widening of structures. Surprisingly, the replication depth increases with increasing injection velocity up to $4 \text{ cm}^3/\text{s}$ and decreases for higher injection velocities. The width of the holes was not found to vary with the injection velocity. We expected the replication depth to increase monotonously with increasing velocity, until reaching the full height of the mold structures, with the caveat that other micro- and macroscale defects like

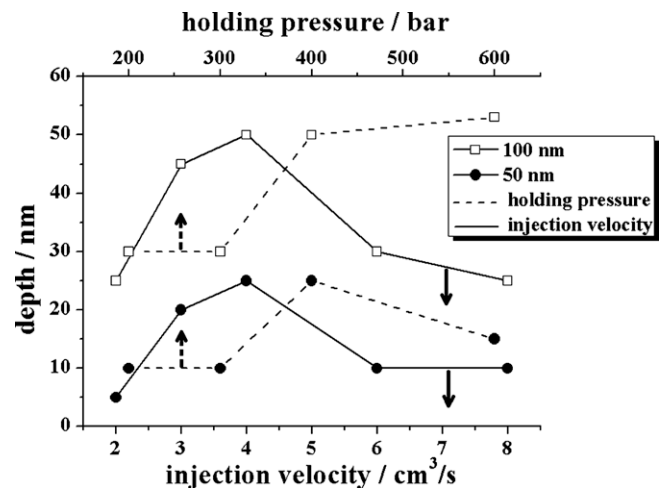


Fig. 3. Replication depth of 50 and 100 nm wide holes (mold: 58 nm high pillar structures) as a function of injection velocity (lower axis; holding pressure: 400 bars) or holding pressure (upper axis; injection speed: $4 \text{ cm}^3/\text{s}$) at a mold temperature of 125°C and a melt temperature of 260°C .

warping and microcracks can appear at very high injection velocities. We currently explore the phenomenon of a maximum replication depth at intermediate velocities in more detail.

Variation in mold and melt temperature in the range explored showed no substantial influence on the replication fidelity. However, different research groups have shown that the replication depth can be improved by increasing melt and mold temperature, increasing injection velocity, as well as increasing the injection and holding pressure [5,7].

3.3. Bonding

Microfluidic chip parts and nanostructure chip parts, both injection molded in Topas 5013 were successfully thermally bonded. The bonding process caused a deformation of the whole area covering the microfluidic channel of about 2 μm in the channel center. The deformation of the nanostructures itself was analyzed by SEM after forced mechanical debonding. No measurable deformation was observed (Fig. 2d).

4. Conclusion

Injection molding is capable of mass producing arrays of nano-holes of 50 nm width and 35 nm in depth as well as 100 nm wide holes replicated to the full depth of 105 nm (Fig. 2c). The application of a fluorocarbon based antistiction coating improves the replication fidelity of shape and depth substantially. The coating did not cause any observable reduction in replication depth. Optimized process parameters, i.e. injection velocity and holding pressure, allow the fabrication of highly ordered nanostructures of controlled size with an aspect ratio of at least unity for structures 100 nm in width. Nanoscale features can be integrated in a polymer microflu-

idic system without substantial deformation of the structures though the overall surface may bend slightly during thermal bonding. We believe that further optimization of injection molding and bonding parameters and application of antistiction coatings may permit for smaller nanostructures with even higher aspect ratios and their registry to a microfluidic system.

Acknowledgements

This work was supported by The Danish Research Council for Technology and Production Sciences Grant No. 26-04-0074. We would like to thank J. Pedersen and A. Møller, DVD Norden A/S, for preparing the electroplated nickel replicas, as well as P. Shi for many useful discussions and continuous support with the electron beam lithography.

References

- [1] G. Xie et al., *Nanotechnology* 19 (2008) 095605.
- [2] C.-J. Ting et al., *Journal of Micromechanics and Microengineering* 18 (2008) 075001.
- [3] H.-K. Koponen et al., *Applied Surface Science* 253 (2007) 5208–5213.
- [4] M.J. Dalby et al., *Nature Materials* 6 (2007) 997–1003.
- [5] C.K. Huang, *Journal of Micromechanics and Microengineering* 17 (2007) 1518.
- [6] D. Macintyre, S. Thom, *Microelectronic Engineering* 41/42 (1998) 211.
- [7] K. Mönkkönen et al., *Polymer Engineering Science* 42 (2002) 1600.
- [8] H. Schiff et al., *Microelectronics and Engineering* 53 (2000) 171–174.
- [9] H. Pranov et al., *Polymer Engineering Science* (2006) 160.
- [10] H. Schiff, A. Kristensen, *Nanoimprint lithography*, in: B. Bhushan (Ed.), *Springer Handbook of Nanotechnology*, second ed., Springer, Berlin, 2007, pp. 239–278.
- [11] Y. Guo, *Microsystem Technology* 13 (2007) 411–415.
- [12] N. Lee et al., *Applied Physics Letter* 88 (2006) 073101.
- [13] H. Pranov, Ph.D. Thesis, Technical University of Denmark, 2006.